Iterative global sensitivity analysis algorithm with neural network surrogate modeling

Yen-Chen Liu[1][0000−0003−1769−9738], Jethro Nagawkar[1][0000−0002−3653−4720], Leifur Leifsson[1][0000−0001−5134−870X], Slawomir Koziel[2,3][0000−0002−9063−2647], and Anna Pietrenko-Dabrowska[3][0000−0003−2319−6782]

[1] Department of Aerospace Engineering, Iowa State University, Ames IA 50011, USA
{clarkliu,jethro,leifur}@iastate.edu
[2] Engineering Modeling & Optimization Center, School of Science and Engineering, Reykjavik University, Menntavegur 1, 101 Reykjavik, Iceland
koziel@ru.is
[3] Faculty of Electronics Telecommunications and Informatics, Gdansk University of Technology, Narutowicza 11/12, 80-233 Gdansk, Poland
anna.dabrowska@pg.edu.pl

Abstract. Global sensitivity analysis (GSA) is a method to quantify the effect of the input parameters on outputs of physics-based systems. Performing GSA can be challenging due to the combined effect of the high computational cost of each individual physics-based model, a large number of input parameters, and the need to perform repetitive model evaluations. To reduce this cost, neural networks (NNs) are used to replace the expensive physics-based model in this work. This introduces the additional challenge of finding the minimum number of training data samples required to train the NNs accurately. In this work, a new method is introduced to accurately quantify the GSA values by iterating over both the number of samples required to train the NNs, terminated using an outer-loop sensitivity convergence criteria, and the number of model responses required to calculate the GSA, terminated with an inner-loop sensitivity convergence criteria. The iterative surrogate-based GSA guarantees converged values for the Sobol' indices and, at the same time, alleviates the specification of arbitrary accuracy metrics for the surrogate model. The proposed method is demonstrated in two cases, namely, an eight-variable borehole function and a three-variable nondestructive testing (NDT) case. For the borehole function, both the first- and total-order Sobol' indices required 200 and 10^5 data points to terminate on the outer- and inner-loop sensitivity convergence criteria, respectively. For the NDT case, these values were 100 for both first- and total-order indices for the outer-loop sensitivity convergence, and 10^6 and 10^3 for the inner-loop sensitivity convergence, respectively, for the first- and total-order indices, on the inner-loop sensitivity convergence. The differences of the proposed method with GSA on the true functions are less than 3% in the analytical case and less than 10% in the physics-based case (where the large error comes from small Sobol' indices).

Keywords: Global sensitivity analysis · surrogate modeling · neural networks · Sobol' indices · termination criteria.

ICCS Camera Ready Version 2021
To cite this paper please use the final published version:
DOI: 10.1007/978-3-030-77970-2_23

1 Introduction

Sensitivity analysis (SA) [1, 2] plays an important role in engineering, design, and analysis. SA quantifies the effects of individual input parameters, as well as combinations of input parameters, on the output model response [3, 4]. Engineers and scientists can use SA in deciding which parameters are important while performing experimental or computational studies. SA can be classified as either local [5] or global [6] SA. In local SA, small perturbations in the inputs are used to quantify its effects on the output model response. In global SA, the variance of output model response due to the input variability is quantified. This work focuses on global variance-based SA with Sobol' indices [3, 4].

Model-based SA often relies on using high-fidelity physics-based models. The use of such model-based SA can be challenging due to a variety of reasons, including (1) the physics-based models can be computationally costly to solve, (2) engineering problems can require a large number of variability parameters, and (3) SA requires multiple and repetitive physics-based model evaluations. The combination of these challenges may result in problems that are difficult to solve in a reasonable amount of time.

To reduce this computational burden, surrogate modeling methods [7] can be used. Surrogate models replace the high-fidelity physics-based models with a computationally efficient ones. Surrogate models (also called metamodels) can be broadly classified as either data-fit methods [7] or multifidelity methods [8]. In data-fit methods, a response surface is fitted through the responses of evaluated high-fidelity models. Examples include Kriging [9], neural networks (NN) [10], and support vector machines [11]. In multifidelity methods, data from multiple levels of fidelity are fused together to make predictions on the level of the high-fidelity model. Examples of multifidelity modeling methods include Cokriging [12] and manifold mapping [13]. This work utilizes data-fit surrogate modeling, namely NNs, in lieu of the high-fidelity physics-based models within a GSA framework.

In this paper, a new approach for surrogate-based GSA with Sobol' indices [3] is proposed. Specifically, in the proposed surrogate framework, the number of samples used to train the NNs is iteratively increased. The goal of the proposed algorithm is twofold: to minimize the training cost of the NNs while still yielding converged Sobol' indices and alleviating the specification of arbitrary surrogate modeling accuracy metrics. The latter is important because accuracy metrics for surrogate models do not guarantee that converged Sobol' indices are obtained.

The remainder of the paper is organized as follows. Next section gives the details of the proposed method, including the GSA framework with surrogate modeling, the procedure of iteratively improving sensitivity results, and the convergence criteria for termination. The following section describes the results of two numerical examples benchmarking the sensitivity results of the proposed method against the actual sensitivity. The last section concludes the paper and discusses potential future work.

ICCS Camera Ready Version 2021
To cite this paper please use the final published version:
DOI: 10.1007/978-3-030-77970-2_23

2 Methods

This section describes a general SA problem and the proposed algorithm, including the iterative approach, the surrogate modeling, the Sobol' analysis, and the convergence of the algorithm.

2.1 Problem statement

Quantifying the effects of the inputs on the output response of a system or model is essential for making design and engineering decisions. Global SA using Sobol' indices [3] is one such method of quantifying the variance of the model output due to variability in the inputs to the model. In this work, the physics-based models are considered as black box functions described as

$$y = f(\mathbf{x}), \tag{1}$$

where $\mathbf{x} \in \mathbb{R}^D$ is a set of D-dimensional input parameters and a single output y. The model output is perturbed due to probabilistically distributed random inputs, which imitate the uncertainties from different sources. This work proposes a method to determine the sensitivity of each input variability parameter on the model output. The following sections give a detailed explanation of the methodology used in this work.

2.2 Iterative global sensitivity analysis workflow

Figure 1 demonstrates the proposed method. The process starts by taking a small population of samples from the uncertainty input parameters. Samples are selected randomly from each probability distribution of the inputs via the Latin hypercube sampling (LHS) [14] method. The simulation model then generates the corresponding outputs and uses them as training data to construct a surrogate model that mimics the same input-output behavior of the simulation model. The surrogate modeling method used in this work is discussed in the next section. GSA is then performed with this surrogate model using Sobol' indices, and the local and global convergence of these indices are checked. In the inner-loop, the current surrogate model is used to calculate the Sobol' indices, and the number of samples is increased by one order of magnitude during each iteration until local convergence is achieved. The precision of the GSA is affected by the predicted outputs from the surrogate model, which is usually related to the number of physics-based model training samples. Therefore, to estimate the global convergence of the Sobol' indices, the above process is resampled with an increasing number of training data samples from the physics-based model in the outer-loop until convergence criteria are met. The outcome yields the converged Sobol' indices and the corresponding surrogate model.

ICCS Camera Ready Version 2021
To cite this paper please use the final published version:
DOI: 10.1007/978-3-030-77970-2_23

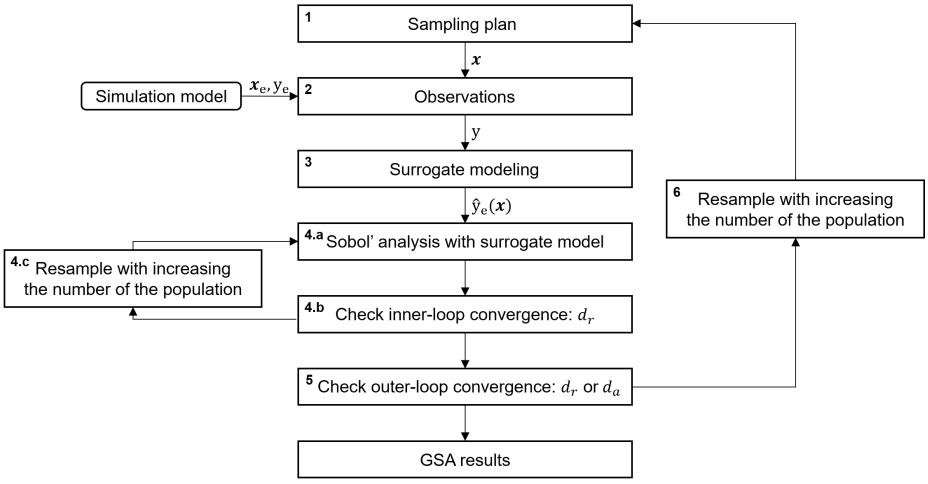

Fig. 1: A flowchart of the surrogate-based iterative global sensitivity analysis algorithm.

2.3 Surrogate modeling with neural networks

NNs are a subclass of surrogate models where any function can be approximated through a hierarchy of features [10]. Layers are steps in this hierarchy of features [15]. The layers in-between the input and output layers are called hidden layers [16]. An architecture of an NN is shown in Fig. 2. This NN has two hidden layers as well as an input and output layer. The input and output layers have six inputs and three outputs, respectively. The choice of the number of inputs and outputs is problem dependant, where this value is equal to the number of independent (input) variables and dependant (output) variables of the problem being solved. The output and hidden layers each consist of neurons. In a NN, neurons are fundamental units of computation [10]. Neurons output nonlinear transformations of a weighted sum of the outputs from a previous hidden or input layer[10]. This nonlinear transformation is termed activation [15]. Changing the number of hidden layers and the number of neurons in each hidden layer affects the complexity of the function being approximated [10].

The activation function in each neuron of a given hidden layer, L, is given by [10]

$$z_j^{(L)} = a\Big(\sum_{i=1}^{N^{(L-1)}} \omega_{ji}^{(L)} z_i^{(L-1)} + b^{(L-1)}\Big), \tag{2}$$

where $N^{(L-1)}$ refers to the number of neurons in the $L-1$ hidden layer, while $z_j^{(L-1)}$ and $z_i^{(L)}$ are the outputs of the j^{th} and i^{th} neurons, respectively, in the L and $L-1$ hidden layers, respectively. The activation function is denoted by a, the weight between the i^{th} neuron in the $L-1$ hidden layer and the j^{th} neuron in the L hidden layer is denoted by $\omega_{ji}^{(L)}$, and the bias unit in the $L-1$ hidden

ICCS Camera Ready Version 2021
To cite this paper please use the final published version:
DOI: 10.1007/978-3-030-77970-2_23

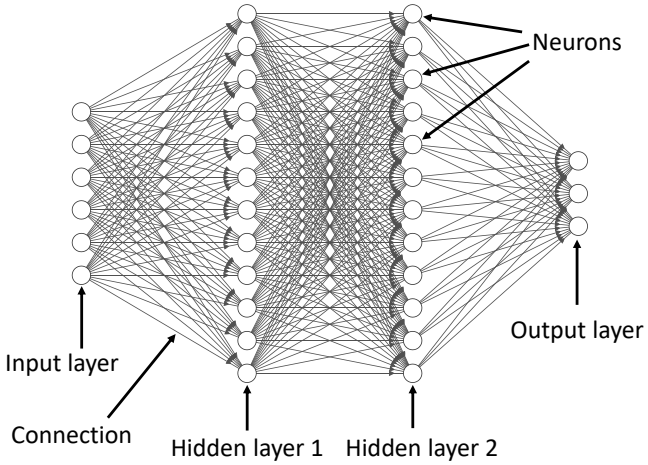

Fig. 2: A schematic of a neural network.

layer is denoted by $b^{(L-1)}$. These weight and biases are termed parameters of the NN. To tune these parameters, an optimization problem is solved to reduce the loss function ($\mathcal{L}$) with respect to all the parameters of the NN. The Adaptive Moments (ADAM) [17] gradient-based optimizer [10] is used to find the values of these parameters, and the backpropagation algorithm [18] is used to find the gradients.

The loss function is defined to capture the mismatch between the training data observations, y, and the predicted, $\hat{y}$, of the NN. In this work, the mean squared error (MSE) along with a L_2 regularization term, averaged over all the training data, is used and is given by

$$\mathcal{L} = \frac{\sum_{l=1}^{N_{tr}} \sum_{m=1}^{N_o} (\hat{y}_m^{(l)} - y_m^{(l)})^2}{N_{tr} N_o} + \lambda \frac{\sum_{n=1}^{N_w} (W_n)^2}{2N_{tr}}, \tag{3}$$

where the first half of the equation represents the MSE, and the second half is the L_2 regularization term. The L_2 regularization term is an additional term added to prevent the NN from overfitting the training data [10]. N_o is the size of the output layer, N_{tr} is the number of training data sets, N_w is the total number of parameters (W) in the NN, l is the index of the training data-set, m is the index of the neuron in the output layer, and λ is the regularization constant. In practice, a subset of the training data, called mini-batch [10], is used to calculate the loss function.

To tune the hyperparameters of the NN, a testing set of $1,000$ samples is used. These hyperparameters are varied till both the training and testing loss values are of a similar order of magnitude and as low as possible. The common hyperparameter values for the cases selected in this study are the tangent hyperbolic function, a learning rate of 0.001, 100 neurons in each hidden layer, a mini-batch size of 16, and a maximum number of epochs of $2,000$. For the

ICCS Camera Ready Version 2021
To cite this paper please use the final published version:
DOI: 10.1007/978-3-030-77970-2_23

borehole case, the number of hidden layers was set to two, and the λ value was set to 0.1. For the NDE case, these values were set to one and 0.01, respectively. Definitions for these hyperparameters can be found in [10].

2.4 Sobol' indices

In this study, the global variance-based sensitivity analysis with Sobol' indices [3, 4] is used. It is used to quantify the effect of each individual inputs as well combination of inputs on the output model response. Given a model $y = f(\mathbf{x})$, where $\mathbf{x}$ is a set of D input parameters and y is the model output, it can be decomposed into the following form [4]

$$y = y_0 + \sum_{i=1}^{D} y_i + \sum_{i<j}^{D} y_{ij} + ... + y_{1,2,...,D}, \tag{4}$$

where y_0 is a constant, y_i is the model output from varying individual x_i's, y_{ij} is the model output from varying x_i and x_j simultaneously, and so on. The total variance of y measures how far the uncertainties of the model inputs propagating to the model output, and the right-hand side of (4) becomes

$$\mathrm{Var}(y) = \sum_{i=1}^{D} V_i + \sum_{i<j}^{D} V_{ij} + ... + V_{12...D}, \tag{5}$$

where

$$V_i = \mathrm{Var}_{x_i}(E_{\mathbf{x}_{\sim i}}(y|x_i)), \tag{6}$$

$$V_{ij} = \mathrm{Var}_{x_{ij}}(E_{\mathbf{x}_{\sim ij}}(y|x_i, x_j)) - V_i - V_j, \tag{7}$$

and so on. $\mathbf{x}_{\sim i}$ represents all the variables except x_i. V_i represents the variance of the output due to individual x_i, while V_{ij} is the variance of the output due to interaction between x_i and x_j. Dividing equation (5) by $\mathrm{Var}(y)$ results in

$$1 = \sum_{i=1}^{D} S_i + \sum_{i<j}^{D} S_{ij} + ... + S_{12...D}, \tag{8}$$

where the main effect indices, also known as first-order Sobol's indices [4] are given by

$$S_i = \frac{V_i}{\mathrm{Var}(y)} = \frac{\mathrm{Var}_{x_i}(E_{\mathbf{x}_{\sim i}}(y|x_i))}{\mathrm{Var}(y)}, \tag{9}$$

where S_i is the contribution of individual x_i on the output model variance. The total-effect Sobol' indices [4] are given by

$$S_{T,i} = 1 - \frac{\mathrm{Var}_{\mathbf{x}_{\sim i}}(E_{x_i}(y|\mathbf{x}_{\sim i}))}{\mathrm{Var}(y)}, \tag{10}$$

where $S_{T,i}$ measures the contribution of both individual x_i and the interaction between x_i and other model input parameters.

ICCS Camera Ready Version 2021
To cite this paper please use the final published version:
DOI: 10.1007/978-3-030-77970-2_23

2.5 Convergence criterion

The proposed iterative method includes an outer-loop that samples the physics-based model to train the surrogate NN models and an inner-loop that computes the Sobol' indices by sampling the trained NN surrogate model. Both the inner- and outer-loop are terminated based on the convergence of the Sobol' indices between successive iterations.

The inner-loop convergence is measured by the absolute relative change of Sobol' indices defined as

$$d_r[s_i] = \left| \frac{s_i^{(\mathrm{n})} - s_i^{(\mathrm{n}-1)}}{s_i^{(1)}} \right|, \tag{11}$$

where n represents the current iteration index, i represents the index of input parameter, and s represents the value of the Sobol' indices and is calculated separately for first- and total-order indices. The inner-loop is terminated when $d_r[s_i] \leq \epsilon_r$ for all s_i. In this work, ϵ_r is set to 0.1.

Convergence of the outer-loop is measured by (11) and the absolute change of Sobol' indices, given by

$$d_a[s_i] = \left| s_i^{(\mathrm{m})} - s_i^{(\mathrm{m}-1)} \right|, \tag{12}$$

where m represents the current iteration index. The outer-loop is terminated when $d_r[s_i] \leq \epsilon_r$ or $d_a[s_i] \leq \epsilon_a$ for all s_i. In this work, ϵ_a is set to 0.01.

3 Numerical Examples

This section presents two numerical problems; an analytical function and a physics-based system solved using the proposed method for GSA. Both cases involve multiple uncertainty input parameters in the computations, which usually require running numerous repetitive evaluations directly on the true function for GSA calculations.

3.1 Case 1: Analytical function

The analytical function used in this study is the eight variable borehole function [19]. The borehole function is used to model the flow of water through a borehole and is given by

$$f_{\mathrm{HF}} = \frac{2\pi T_u (H_u - H_l)}{ln(r/r_w)\left(1 + \frac{2LT_u}{ln(r/r_w) r_w^2 K_w} + \frac{T_u}{T_l}\right)}, \tag{13}$$

where r_w and r are the radius of the borehole and the radius of influence of the borehole, respectively, T_u and T_l are the transmissivity of the upper and lower aquifer, respectively, H_u and H_l are the potentiometric head of upper and lower aquifers, respectively, L is the length of the borehole, and K_w is the hydraulic

ICCS Camera Ready Version 2021
To cite this paper please use the final published version:
DOI: 10.1007/978-3-030-77970-2_23

conductivity of the borehole. Each of the variability parameters along with their units and distributions are given in Table. 1.

Performing GSA with the proposed method starts by drawing 10 LHS samples and producing borehole function outputs to train the NN. Once trained, this NN model is then sampled to compute the Sobol' indices within the inner-loop. For this inner-loop, the NN is first sampled using 10^2 samples and these samples are increased by one order of magnitude during each iteration of the inner-loop until the convergence criterion of $d_r \leq \epsilon_r$ is met. This is done separately for both first- and total-order Sobol' indices and an example of the convergence plots are shown in Figs. 3(a) and 3(b), respectively. This process is continued by increasing the sample population to 50 in the global loop and by repeating the previous steps. The outer-loop termination criteria are checked between the converged Sobol' indices of the NN models trained with 10 and 50 samples and are shown in Figs. 4(a) and 4(b) for the first- and total-order Sobol' indices, respectively.

Table 1: Variability parameters and their corresponding distribution of the borehole function [19].

Variability Parameters	**Distribution**
Radius of borehole, $r_w(m)$	$N(0.1, 0.0161812^2)$
Radius of influence, $r(m)$	$LogN(7.71, 1.0056^2)$
Transmissivity of upper aquifer, $T_u(m^2/yr)$	$U(63070, 115600)$
Potentiometric head of upper aquifer, $H_u(m)$	$U(990, 1110)$
Transmissivity of lower aquifer, $T_l(m^2/yr)$	$U(63.1, 116)$
Potentiometric head of lower aquifer, $H_l(m)$	$U(700, 820)$
Length of borehole, $L(m)$	$U(1120, 1680)$
Hydraulic conductivity of borehole, $K_w(m/yr)$	$U(9855, 12045)$

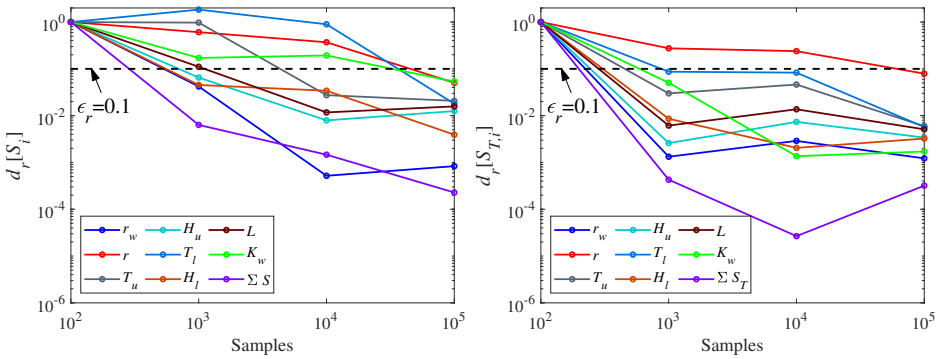

Fig. 3: Case 1 inner-loop convergence of s_i for the NN trained with 200 LHS samples: (a) first-order indices, and (b) total-order indices.

ICCS Camera Ready Version 2021
To cite this paper please use the final published version:
DOI: 10.1007/978-3-030-77970-2_23

The entire process is repeated by increasing the number of samples required to train the NN, until the outer-loop convergence criteria of either $d_r \leq \epsilon_r$ or $d_a \leq \epsilon_a$ is met.

For the borehole function, the NN needs to be trained with 200 samples until these criteria are met for both the first- and total-order indices. The converged Sobol' indices are displayed in Fig. 5. The GSA results from the proposed method are compared to the Sobol' indices computed by directly sampling the borehole function and is shown in Table 2. The radius of influence of the borehole, as well as the transmissivity of the upper and lower aquifers have negligible influence on the output response (flow rate) of the borehole, while the radius of the borehole has the highest impact on the flow rate.

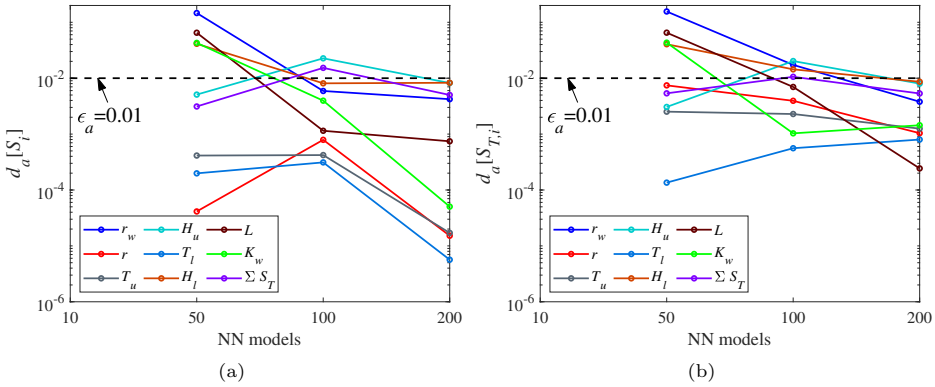

Fig. 4: Case 1 outer-loop convergences of s_i terminated on $d_a \leq \epsilon_a$ criteria: (a) first-order indices, and (b) total-order indices.

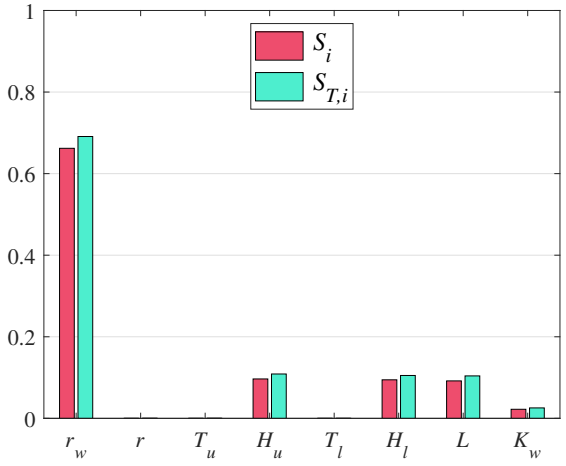

Fig. 5: Case 1 Sobol' index values of input parameters computed by the converged NN model.

ICCS Camera Ready Version 2021
To cite this paper please use the final published version:
DOI: 10.1007/978-3-030-77970-2_23

Table 2: Case 1 comparison of Sobol' index values calculated by sampling the borehole function directly and by sampling the converged NN model.

x	S_i			$S_{T,i}$		
	true function	NN model	% error	true function	NN model	% error
r_w	0.6638	0.6621	0.3%	0.6941	0.6910	0.4%
r	0	0	-	0	0.0002	-
T_u	0	0	-	0	0.0002	-
H_u	0.0949	0.0966	1.7%	0.1061	0.1088	2.5%
T_l	0	0	-	0	0	-
H_l	0.0948	0.0945	0.3%	0.1061	0.1051	0.9%
L	0.0907	0.0918	1.2%	0.1028	0.1041	1.3%
K_w	0.0219	0.0222	1.4%	0.0251	0.0256	2.0%

3.2 Case 2: Ultrasonic nondestructive testing

This study uses the spherically-void-defect under focused transducer ultrasonic (UT) nondestructive testing (NDT) benchmark case. This case was developed by the World Federal Nondestructive Evaluation Center [20]. The main goal of this case is to find the minimum number of training data required to accurately predict the Sobol' Indices using NN as well as quantify the contribution of each variability parameter on the output model response.

Figure 6 shows the setup for the UT benchmark case used in this study. The variability parameters considered for this case are the probe angle (θ), the x location of the probe (x), and the F-number (F). The distributions of each of these parameters are shown in Table. 3.

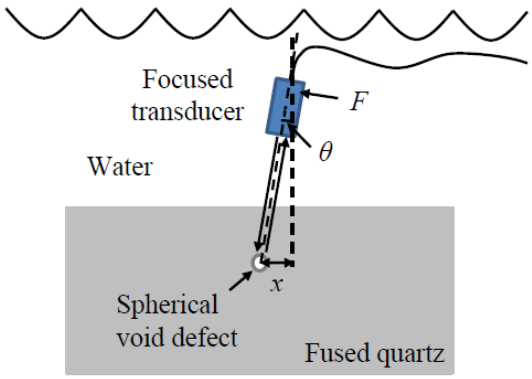

Fig. 6: Setup for the ultrasonic testing case.

ICCS Camera Ready Version 2021
To cite this paper please use the final published version:
DOI: 10.1007/978-3-030-77970-2_23

To predict the voltage waveforms at the receiver, the Thompson-Grey model [21] is used, while the velocity diffraction coefficient is calculated using the multi-Gaussian beam model [22]. Closed-form expressions of the scattering amplitude can then be calculated using the separation of variables [23]. In this study, a center frequency of 5 MHz is used for the transducer. The density of the fused quartz block is set to $2,000\ kg/m^3$, while the longitudinal and shear wave speeds are set to $5,969.4\ m/s$ and $3,774.1\ m/s$, respectively. More information about this model can be found in Du et al. [24].

A similar approach to the previous case is used for this case. The same convergence criteria were used in this case as in the previous case. The outer-loop iterated from 10 to 100 LHS samples, and the convergence plots for the first- and total-order indices are shown in Figs. 8(a) and 8(b), respectively. The convergence plots for the inner-loop of the first- and total-order indices of the trained 100 NN model are shown in Figs. 7(a) and 7(b), respectively. Both the first- and total-order indices require 100 samples each to terminate the outer-loop. The first-order indices require 10^6 samples to terminate the inner-loop, while the total-order indices require 10^3. Figure 9 shows that the F-number has a negligible effect on the output response, while the probe angle has the highest effect. Table 4 compares the Sobol' indices values from the proposed method to those from the true function, showing a good match.

Table 3: Variability parameters and their distribution for the ultrasonic testing case

Variability Parameters	Distribution
θ (deg)	$N(0,\ 0.5^2)$
x (mm)	$U(0,\ 1)$
F	$U(13,\ 15)$

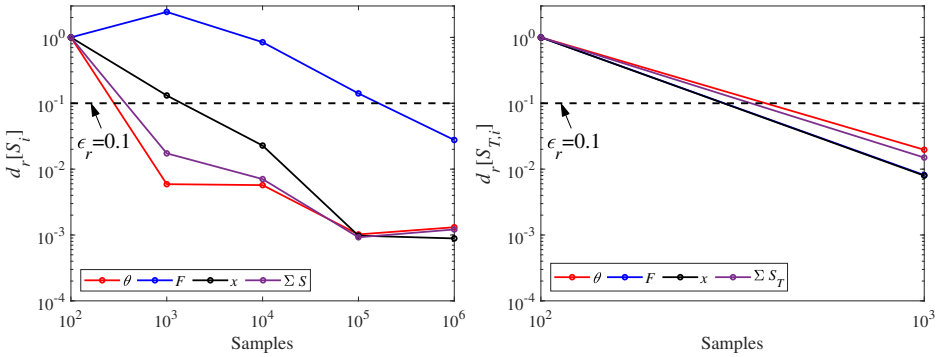

Fig. 7: Case 2 inner-loop convergence of s_i for the NN trained with 100 LHS samples: (a) first-order indices, and (b) total-order indices.

ICCS Camera Ready Version 2021
To cite this paper please use the final published version:
DOI: 10.1007/978-3-030-77970-2_23

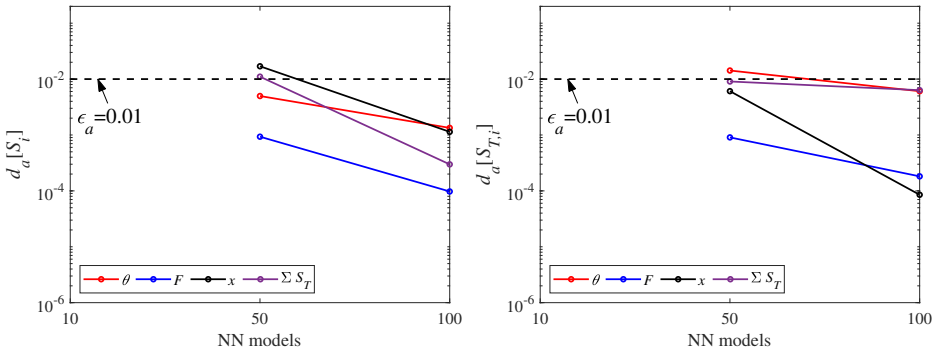

Fig. 8: Case 2 outer-loop convergence of s_i terminated on $d_a \leq \epsilon_a$ criteria: (a) first-order indices, and (b) total-order indices.

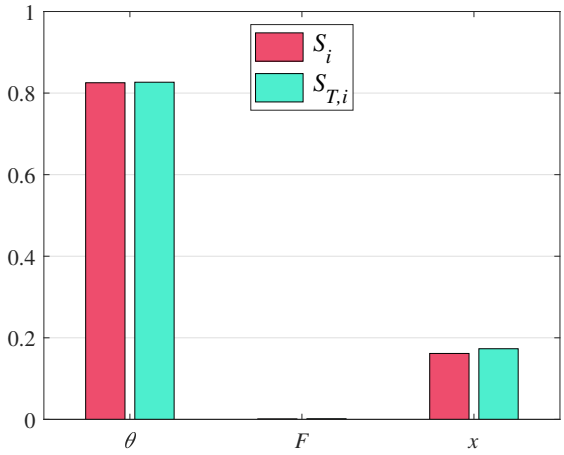

Fig. 9: Case 2 Sobol' index values of input parameters computed by the converged NN model.

Table 4: Case 2 comparison of Sobol' index values between the true model and the converged NN model.

x	S_i			$S_{T,i}$		
	true model	NN model	% error	true model	NN model	% error
θ	0.8269	0.8253	0.2%	0.8367	0.8266	1.2%
F	0.0011	0.0010	9.1%	0.0014	0.0013	7.1%
x	0.1622	0.1616	0.4%	0.1732	0.1732	0%

ICCS Camera Ready Version 2021
To cite this paper please use the final published version:
DOI: 10.1007/978-3-030-77970-2_23

4 Conclusion

This work has presented an algorithm for global sensitivity analysis (GSA) by evaluating Sobol' indices iteratively with surrogate modeling. The goal of the proposed approach is to obtain accurate GSA results while using few evaluations for the true model. Furthermore, the proposed method avoids the specification of arbitrary surrogate modeling accuracy metrics. The efficacy of the proposed algorithm is demonstrated using an analytical function and a physics-based model and comparing against the Sobol' indices obtained with the true functions. The results show that accurate and fully converged Sobol' indices can be achieved at a low computational cost. Future research will benchmark the computational cost and the accuracy of the proposed algorithm against other GSA and surrogate modeling techniques.

Acknowledgements

This material is based upon work supported by the U.S. National Science Foundation under grants no. 1739551 and 1846862, as well as by the Icelandic Centre for Research (RANNIS) grant no. 174573053.

References

1. Ferretti, F., Saltelli, A., Tarantola, S.: Trends in Sensitivity Analysis Practice in the Last Decades. Science of the Total Environment **568**, 666–670 (2016). https://doi.org/10.1016/j.scitotenv.2016.02.133
2. Iooss, B., Saltelli, A.: Introduction to Sensitivity Analysis. Springer International Publishing, Switzerland, 2015 (2015)
3. Sobol', I., Kucherekoand, S.: Sensitivity estimates for nonlinear mathematical models. Mathematical Modelling and Computational Experiments **1**, 407–414 (1993)
4. Sobol', I.: Global sensitivity indices for nonlinear mathematical models and their monte carlo estimates. Mathematics and Computers in Simulation **55**, 271–280 (2001)
5. Zhou, X., Lin, H.: Local Sensitivity Analysis. Encyclopedia of GIS pp. 1116–1119 (2017)
6. Homma, T., Saltelli, A.: Importance Measures in Global Sensitivity Analysis of Nonlinear Models. Reliability Engineering and System Safety **52**, 1–17 (1996)
7. Forrester, A.I.J., Keane, A.J.: Recent Advances in Surrogate-Based Optimization. Progress in Aerospace Sciences **45**(1-3), 50–79 (2009). https://doi.org/10.1016/j.paerosci.2008.11.001
8. Peherstorfer, B., Willcox, K., Gunzburger, M.: Survey of Multifidelity Methods in Uncertainty Propagation, Inference, and Optimization. Society for Industrial and Applied Mathematics **60**(3), 550–591 (2018). https://doi.org/https://doi.org/10.1137/16M1082469
9. Krige, D.G.: A Statistical Approach to Some Basic Mine Valuation Problems on the Witwatersrand. Journal of the Chemical, Metallurgical and Mining Engineering Society of South Africa **52**(6), 119–139 (1951)

ICCS Camera Ready Version 2021
To cite this paper please use the final published version:
DOI: 10.1007/978-3-030-77970-2_23

10. Goodfellow, I., Bengio, Y., Courville, A.: Deep Learning. The MIT Press, Cambridge, MA (2016)
11. Li, D., Wilson, P.A., Jiong, Z.: An Improved Support Vector Regression and Its Modelling of Manoeuvring Performance in Multidisciplinary Ship Design Optimization. International Journal of Modelling and Simulation **35**, 122–128 (2015)
12. Kennedy, C.M., O'Hagan, A.: Predicting the Output from a Complex Computer Code When Fast Approximations are available. Biometrika **87**(1), 1–13 (2000). https://doi.org/10.1093/biomet/87.1.1
13. Echeverria, D., Hemker, P.: Manifold mapping: A two-level optimization technique. Computing and Visualization in Science **11**, 193–206 (2008). https://doi.org/10.1007/s00791-008-0096-y
14. McKay, M.D., Beckman, R.J., Conover, W.J.: A comparison of three methods for selecting values of input variables in the analysis of output from a computer code. Technometrics **21**(2), 239–245 (1979), http://www.jstor.org/stable/1268522
15. Haykin, S.S.: Neural networks and learning machines. Pearson Education, Upper Saddle River, NJ, 3^{rd} edn. (2009)
16. Schmidhuber, J.: Deep learning in neural networks: An overview. Neural Networks **61**, 85 – 117 (2015). https://doi.org/10.1016/j.neunet.2014.09.003
17. Kingma, D.P., Ba, J.: Adam: A method for stochastic optimization. arXiv:1412.6980 (2014)
18. Chauvin, Y., Rumelhart, D.E.: Backpropagation: theory, architectures, and applications. Psychology press, Hillsdale, NJ (1995)
19. Harper, W.V., Gupta, K.S.: Sensitivity/uncertainty analysis of a borehole scenario comparing Latin Hypercube Sampling and deterministic sensitivity approaches. Technical report, Office of Nuclear Waste Isolation, Columbus, OH (1983)
20. Gurrala, P., Chen, K., Song, J., Roberts, R.: Full wave modeling of ultrasonic NDE benchmark problems using Nystrom method. Review of Progress in Quantitative Nondestructive Evaluation **36**(1), 1–8 (2017)
21. Schmerr, L., Song, J.: Ultrasonic Nondestructive Evaluation Systems. Springer Science + Business Media, LLC, New York, USA (2007)
22. Wen, J.J., Breazeale, M.A.: A Diffraction Beam Field Expressed as the Superposition of Gaussian Beams. The Journal of the Acoustical Society of America **83**, 1752–1756 (1988)
23. Schmerr, L.: Fundamentals of Ultrasonic Nondestructive Evaluation: A Modeling Approach. Springer Science & Business Media (2013)
24. Du, X., Leifsson, L., Meeker, W., Gurrala, P., Song, J., Roberts, R.: Efficient Model-Assisted Probability of Detection and Sensitivity Analysis for Ultrasonic Testing Simulations Using Stochastic Metamodeling. Journal of Nondestructive Evaluation, Diagnostics and Prognostics of Engineering Systems **2(4): 041002**(4) (09 2019), https://doi.org/10.1115/1.4044446

ICCS Camera Ready Version 2021
To cite this paper please use the final published version:
DOI: 10.1007/978-3-030-77970-2_23